



Beauchene, C., Abaid, N., Moran, R., Diana, R. A., & Leonessa, A. (2017). The effect of binaural beats on verbal working memory and cortical connectivity. *Journal of Neural Engineering*, 14(2), [026014]. <https://doi.org/10.1088/1741-2552/aa5d67>

Peer reviewed version

Link to published version (if available):  
[10.1088/1741-2552/aa5d67](https://doi.org/10.1088/1741-2552/aa5d67)

[Link to publication record in Explore Bristol Research](#)  
PDF-document

This is the author accepted manuscript (AAM). The final published version (version of record) is available online via IOP at <http://iopscience.iop.org/article/10.1088/1741-2552/aa5d67/meta;jsessionid=D6FA27C56596E605A6520A56AF45CD37.ip-10-40-1-105#artAbst> . Please refer to any applicable terms of use of the publisher.

## University of Bristol - Explore Bristol Research

### General rights

This document is made available in accordance with publisher policies. Please cite only the published version using the reference above. Full terms of use are available: <http://www.bristol.ac.uk/red/research-policy/pure/user-guides/ebr-terms/>

# The Effect of Binaural Beats on Verbal Working Memory and Cortical Connectivity

Christine Beauchene<sup>1</sup>, Nicole Abaid<sup>2</sup>, Rosalyn Moran<sup>3</sup>, Rachel A. Diana<sup>4</sup>, Alexander Leonessa<sup>1\*</sup>

<sup>1</sup> Center for Dynamic Systems Modeling and Control, Department of Mechanical Engineering, Virginia Polytechnic Institute and State University, Blacksburg, Virginia, United States of America.

<sup>2</sup> Department of Biomedical Engineering and Mechanics, Virginia Polytechnic Institute and State University, Blacksburg, Virginia, United States of America.

<sup>3</sup> Department of Engineering Mathematics, University of Bristol, Clifton, Bristol, UK.

<sup>4</sup> Department of Psychology, Virginia Polytechnic Institute and State University, Blacksburg, Virginia, United States of America.

E-mail: [aleoness@vt.edu](mailto:aleoness@vt.edu)

\* This material is based upon work supported by (while serving at) the National Science Foundation.

December 2016

## Abstract.

**Objective.** Synchronization in activated regions of cortical networks affect the brain's frequency response, which has been associated with a wide range of states and abilities, including memory. A non-invasive method for manipulating cortical synchronization is binaural beats (BB). Binaural beats take advantage of the brain's response to two pure tones, delivered independently to each ear, when those tones have a small frequency mismatch. The mismatch between the tones is interpreted as a beat frequency, which may act to synchronize cortical oscillations. Neural synchrony is particularly important for working memory processes, the system controlling online organization and retention of information for successful goal-directed behavior. Therefore, manipulation of synchrony via BB provides a unique window into working memory and associated connectivity of cortical networks. **Approach.** In this study, we examined the effects of different acoustic stimulation conditions during an N-back working memory task, and we measure participant response accuracy and cortical network topology via EEG recordings. Six acoustic stimulation conditions were used: None, Pure Tone, Classical Music, 5Hz BB, 10Hz BB, and 15Hz BB. **Main results.** We determined that listening to 15Hz BB during an N-Back working memory task increased the individual participant's accuracy, modulated the cortical frequency response, and changed the cortical network connection strengths during the task. Only the 15Hz BB produced significant change in relative accuracy compared to the None condition. **Significance.** Listening to 15Hz BB during the N-back task activated salient frequency bands and produced networks characterized by higher information transfer as compared to other auditory stimulation conditions.

**Keywords:** Binaural beat, Electroencephalography, Graph theory, Working memory

## 1. Introduction

The brain is a highly complex network of nonlinear systems with internal dynamic states that are not easily quantified. As a result, it is essential to understand the properties of the connectivity network linking disparate parts of the brain to ascertain the global functional processes it executes. However, analyzing brain connectivity is a nontrivial task, since the electrical activations that drive the dynamics happen in a three-dimensional volume at small spatial and temporal scales. The networked nature of the brain is highly relevant to different functional tasks, such as memory, which occur in diffuse brain regions. An effective method for presenting multivariate data and monitoring brain networks utilizes brain connectivity graphs. The graphs connecting cortical regions are highly random and modular, but show relatively low heterogeneity. Conserved over all scales, the network characteristics include small world degree distributions, modularity, short path lengths, hub nodes, and hierarchy [1].

The statistical dependencies between observed neuronal population responses, also known as functional connectivity, can be used to determine the edge weights of the brain connectivity graphs. Functional connectivity may be inferred from electroencephalography (EEG), magnetoencephalography (MEG), functional MRI (fMRI), or other time series data. Dynamic coupling is assumed in cases when two regions are not statistically independent [2]. Functional connectivity can be computed on the cellular [3] or the regional level [4,5].

Phase synchronization is a statistical quantity well suited for determining functional connectivity, and thus brain networks, since it measures the interdependence of two oscillators. Such methods have been applied in the fields of nonlinear dynamics and chaotic systems [6] and translate well to EEG since it is noisy, non-linear, and non-stationary [7]. Within the brain, synchronous gamma (25-40Hz) oscillations are confined to local neuronal populations, while theta (4-8Hz) synchronization is found across regions of the brain [8]. Regional interactions associated with memory tasks are reflected in both the theta and gamma EEG oscillatory frequency bands [9–11].

Working memory is the neural system which controls the processing and organization of consciously accessible information for successful reasoning, comprehension, and goal-directed behavior [12, 13]. Humans have a limited capacity with respect to the amount of information that can be simultaneously retained in working memory. Successful maintenance of information in working memory is associated with increased cortical phase synchronization [9, 14, 15]. From a neurophysiological point of view, in both verbal and visuospatial working memory tasks, the bilateral prefrontal (PFC) and posterior parietal (PPC) cortices are activated [16–18]. **Theta phase synchronization during a working memory task is sustained during encoding, maintenance, and retrieval between these two anatomical regions and increases with memory load (difficulty of the task) [9, 19].** Previous neuroimaging data suggests that hemispheric specialization varies with the working memory domain (verbal or visuospatial) such that left lateralized regions are recruited for verbal tasks or right lateralized for visuospatial tasks [20]. Alternatively, it has been proposed that verbal working memory performance relies on successful encoding of a stimulus as both a spatial object in the right hemisphere and a verbal construct in the left hemisphere [16].

A variety of interventions can be used to stimulate the brain at a particular

frequency thereby allowing manipulation of cortical oscillations and subsequent observation of the effects of the manipulation. Current methods of stimulation include electrical signals, magnetic fields, and ultrasound. However, few existing methods are able to be used in concert with traditional neural measurement systems (EEG, MEG, etc.) and almost none take advantage of the brain's own structure to actively generate internal oscillatory modulations. Binaural beats can be used to produce oscillations in the existing auditory pathway and is compatible with traditional neural measurement systems [21,22]. Binaural beats arise from the brain's interpretation of two pure tones, with a small frequency mismatch, delivered independently to each ear. A third phantom binaural beat, whose frequency is equal to the difference of the two presented tones, is produced in the Inferior Colliculus (IC) [23]. The phase difference is projected from the IC to the primary auditory cortex by periodic neural firings specific to the binaural beat frequency [24]. Based on the results of Fitzpatrick *et al*, the auditory cortex experiences the highest amount of synchronization due to binaural beats in the beta band around 16Hz [21]. Binaural beats have been shown to further entrain the frontal and parietal cortices using a variety of binaural beat frequencies [25–28]. In addition, binaural beats, have been shown to influence many different aspects of cognition and mood states, such as attention, memory, creativity, and vigilance [29]. Gamma band 40Hz binaural beats have shown to produce the largest effects on the frequency responses [25,27]. However, binaural beats can influence responses outside their respective frequency band [30] and this effect is poorly characterized. The nonlinear relationship between the binaural beat stimulation and cortical activity means that, for working memory, 40Hz BB may not be optimal. For example, one study by Lane *et al* reported that while listening to binaural beats in the beta frequency range during a 1-back working memory task, the participants showed improvement in target detection, and decreased false alarms, task-related confusion, and fatigue [31]. A recent study by our group has also shown that 15Hz BB can improve accuracy and strengthen key connections in the cortical networks during a visuospatial working memory task [32]. For a literature review on the effects of binaural beats on cortical activity and working memory, refer to [32].

The objective of this experiment is to determine the effects binaural beats have on the recorded EEG frequency responses and cortical connectivity, using graph theory methods, during a cognition task. Specifically, a verbal working memory task was chosen since binaural beats have been shown to activate cortical areas key to working memory, which in turn, impacts performance.

## 2. Materials and Methods

### 2.1. Participants

Thirty-four healthy adults (15 women, 19 men) aged 18 to 46 yr (mean 27.1 yr) participated in this study. Each participant provided written consent after being familiarized with the experimental protocols, which were approved by the Virginia Tech Institutional Review Board. Before the start of the task, participants were tested for corrected-to-normal vision and evaluated their hearing using the American Speech-Language-Hearing Association guidelines. No participants reported any previous neurological or hearing problems.

## 2.2. Auditory Stimulus

Multiple acoustic stimulation conditions were evaluated during the course of the session. The control conditions included 1) None, 2) Pure Tone (R: 240Hz, L: 240Hz), and 3) Classical Music (Vivaldi - Spring). The experimental conditions included 1) 5Hz Binaural Beat (R: 240Hz, L: 245Hz), 2) 10Hz Binaural Beat (R: 240Hz, L: 250Hz), and 3) 15Hz Binaural Beat (R: 240Hz, L: 255Hz). The tones presented to the right and left ears are indicated by R and L, respectively. The binaural beats, 5Hz, 10Hz, and 15Hz, serve as theta, alpha, and beta band stimulation, respectively. The tones were created in Matlab. The stimulus volume, played through stereo headphones (MDR-NC7, Sony), was set by the participants at the start of the session to a comfortably loud level.

## 2.3. EEG Recordings

The EEG data were recorded using a 16 gold cup passive electrode EEG system (OpenBCI, Inc., New York, NY) that was interfaced with LabVIEW. The sampling rate was 128Hz. The chosen 10-20 electrode channel locations [33] were Fp1, Fp2, F7, F8, F3, F4, T3, T4, C3, C4, P3, P4, O1, O2, Fz, Cz. The ear lobes were used for the reference and ground electrodes. Prior to data collection, Ten20 EEG conductive paste (Weaver and Co., Aurora, CO) was used to prepare the electrodes and electrode impedances were verified to be  $< 5 \text{ k}\Omega$ .

## 2.4. N-Back Task

Figure 1 shows the chosen N-Back verbal working memory task. During the task, each letter is encoded and the sequence is retained in the working memory. For each letter presented on the screen, the subject must compare the retained (no longer visible) and current (visible on-screen) letters and indicate when the current letter on the screen matches the letter that occurred “N” steps prior. Individual cognitive differences determine the limit on the ‘load’, or number of letters, that can be successfully maintained and manipulated in this task. Capacity is computed using  $K_C = C(H - F)$ , where C is the load, H is the hit rate (percentage of correctly identified matches), and F is the false alarm rate (percentage of non-matches identified as matches) [34].

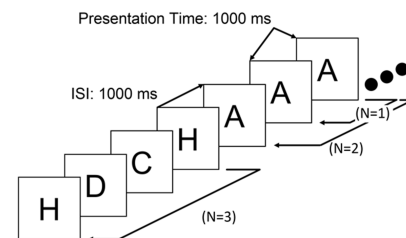


Figure 1: N-back task paradigm.

Individual cognitive differences determine the limit on the ‘load’, or number of letters, that can be successfully maintained and manipulated in this task. Capacity is computed using  $K_C = C(H - F)$ , where C is the load, H is the hit rate (percentage of correctly identified matches), and F is the false alarm rate (percentage of non-matches identified as matches) [34].

Participants completed the N-back test in a quiet, dimly lit room and were seated in front of a computer monitor. A custom script written for the Cogent Graphics Matlab toolbox presented the task. The participant pressed the left arrow or right arrow on the keyboard to indicate a match or no match, respectively. An initial load titration test was completed, before starting the experiment, and involved a practice round (one block of a 1-back task) and then increased in difficulty (one block each of 1-, 2-, and 3-back task). For each participant, the load used in the experimental task was set by selecting the load which produced the highest capacity estimate. In the event that two loads produced identical capacity values, the load with the largest hit rate **less than 100% was used. In case the hit rate equaled 100%, the next highest load was chosen. Each individual was tested at their working memory capacity limit to assess their improvement due to the acoustic stimulation. Of all the participants, thirty-two participants completed the task at a load of 1 and two participants at a load of 2.**

Following the EEG setup, each participant performed the task at the selected load for thirty minutes. The sound condition changed every five minutes to one of the six different acoustic stimulation conditions. The binaural beats began precisely with the first working memory trial of a block and ended with the final trial. Between each block was a two-minute break. Over all participants, all trials and sound conditions were randomized to minimize bias.

### 2.5. Behavioral Data Processing and Analysis

A custom Matlab script was used to process the recorded behavioral data. First, trials were discarded if the participant pressed an incorrect key or didn't respond in time (less than 5%). The metrics used to assess performance during each acoustic stimulation condition were accuracy, ranked accuracy, and reaction time. Accuracy is computed by dividing the the number of correct trials, both matches (Hit) and non-matches (Correct Rejection), by the total number of trials. To identify relative trends in the accuracy results, of each individual participant, a new dataset was constructed by ranking the accuracy of the six sound conditions from 1 (lowest accuracy) to 6 (highest accuracy), for each participant. By ranking each participant's accuracy scores, the data was normalized on a standard scale that eliminated the effect of an individual's mean accuracy. Reaction time is defined as the time observed between when the letter appeared on the screen and when the participant pressed a response button.

The statistical software JMP (SAS, Cary, NC) was used to analyze the behavioral data. The nonparametric Mann-Whitney U statistical test was used since the data ( $N = 34$ ) was non-normal. The post hoc test chosen was the Steel-Dwass All Pairs, which is the nonparametric equivalent to Tukey HSD, and the familywise error rate was kept at a maximum of 0.05. For the behavioral data, CONDITION refers to all acoustic stimulation conditions: None, Pure Tone, Classical, 5Hz BB, 10Hz BB, and 15Hz BB.

### 2.6. EEG Data Processing

The EEGLab toolbox in Matlab was used to preprocess the raw EEG data [35]. Initially, the EEG recordings were bandpass filtered (0.5Hz – 50Hz) to remove drift and the 60Hz power line noise. Then, the filtered EEG was re-referenced to the average. Two different datasets were then derived from the preprocessed EEG data.

The first dataset contains the continuous five-minute block of EEG recordings used for a frequency analysis. First, artifacts were removed using automatic continuous rejection in EEGLab. Then, independent component analysis (ICA) was used to remove the eye blink components [36]. The resulting dataset contained approximately five minutes of clean EEG data, for each condition, for each of the thirty-four participants.

The second dataset contains the epoched EEG used for the graphical network analysis. The onset (0 ms – 1000 ms, which corresponded to the time when the letter was on the screen) epochs were extracted using EEGLab. The onset epoch length remained constant even if the participant responded before the end of the one-second interval. Finally, the baseline was removed (0-200 ms before stimulus presentation). Only correct trials (i.e. a Hit or Correct Rejection) were used. Epochs with artifacts from eye blinks, movement, or other sources were removed following manual inspection of the automatically identified artifacts in EEGLab (less than 5% rejection). The resulting

dataset contained approximately 100 epochs of clean EEG data, for each of the thirty-four participants, for each condition.

### 2.7. Graphical Network Construction

The processed epoched EEG signals were filtered again, using EEGLab, to focus on the theta (4Hz - 8Hz) band (which will be motivated by the results in section 3.2). The time-frequency synchronization measure between channels was computed using the processed EEG signals. The graphical networks are comprised of nodes (the channels) and the edge weights (time-frequency synchronization measure). A measure of synchronization used in the literature is the Phase Locking Value (PLV). The PLV measures the phase coherence between two signals. For example, the PLV of two oscillators is 1 if the phase difference is continually fixed, and is 0 if constantly changing [37]. We compute the PLV using the Matlab Signal Processing Toolbox with the EEG channel recordings converted into analytic signals using a Hilbert transform [38]. Then, the phase, in radians, of the  $h$ th channel in a given epoch is denoted  $\phi_h(t)$ . The phase difference between channel  $h$  and channel  $i$  is given by  $\theta_{hi}(t) = (\phi_h(t) - \phi_i(t)) \bmod 2\pi$ . All pairs of channels are compared against each other via the PLV defined as  $PLV_{hi} = \frac{1}{N} \left[ \sum_{k=0}^N \exp(j\theta_{hi}(k\Delta t)) \right]$ , where  $j = \sqrt{-1}$  is the imaginary unit, and  $\Delta t = \frac{T}{N}$  where  $T$  is the epoch duration and  $N$  is total number of discrete time steps.

The graphical network is constructed using the electrode channels as the nodes ( $V = \{1, \dots, n\}$ ), where  $n = 16$ , and the PLV connection strength is associated with the undirected edges as edge weights ( $E = \{(i, j) : \exists \text{ an edge from } i \text{ to } j\}$ ). The network is undirected and weighted, and can be defined as an adjacency matrix,  $A$ , made up of  $a_{ij}$  elements and a edge weight matrix,  $W$ , made up of  $w_{ij}$  elements. The adjacency matrix has  $a_{ij} = 1$  if  $(i, j) \in E$  and 0 otherwise. The elements of the edge weight matrix are  $w_{ij} = PLV_{ij}$  with the property that  $0 \leq w_{ij} = w_{ji} \leq 1$  for  $i, j = 1, \dots, n, i \neq j$ . Note that both  $A$  and  $W$  are symmetric. **Edge weights in terms of PLV were computed for each epoch and averaged over all epochs to define the graphical network for each participant.**

### 2.8. EEG Analysis

Three different EEG data analyses were undertaken. First, a frequency analysis determined the changes in EEG frequency band power. Second, a graphical network measure analysis determined the modulation of the nodes in the network. Third, the regional connection strengths analysis determined the overall changes in the networks. A power analysis conducted for each EEG analysis determined that greater than 1,000 points were necessary for a power of 0.8 and  $\alpha = 0.05$ . Therefore, we chose to bootstrap the results of each analysis 100 times. The post hoc test chosen was the Tukey HSD, and the familywise error rate was kept at a maximum of 0.05.

**2.8.1. Frequency Band Analysis.** For each condition, for each participant, the theta (4Hz - 8Hz), alpha (8Hz - 12Hz), beta (12Hz - 25Hz), and gamma (25Hz - 40Hz) band FFT power was computed, for each channel. To determine the effect of the stimulation on the frequency response of the EEG, multiple t-tests were computed comparing, for each channel, the None condition against each of the binaural beat stimuli conditions (5Hz, 10Hz, 15Hz). In addition, a two-way factorial ANOVA was used to determine

the effect of the experimental binaural beat stimulation CONDITION (None, 5Hz BB, 10Hz BB, 15Hz BB) and BAND (Theta, Alpha, Beta, Gamma) on the mean FFT power for each channel. Furthermore, looking specifically at Fp1, an electrode placed over a key region involved with verbal working memory, a one-way ANOVA was performed to analyze the effect of CONDITION on the bootstrapped FFT band power.

*2.8.2. Graphical Network Analysis.* Functional networks built from neuroimaging data can be quantified using traditional graphical network metrics [39, 40]. The networks were analyzed using the degree metric computed by the Brain Connectivity Toolbox (BCT) in Matlab. The degree of the  $i$ th node, denoted  $D_i$ , is the sum of the edge weights connected to the node. It measures the amount of information arriving at the node from other regions, and is computed as  $D_i = \sum_{j=1}^n w_{ij}$  with  $n = 16$  the number of channels. Multiple ANOVAs were completed to analyze the degree at the channel and hemispheric level. For this analysis, “regions” refers to the average of the surface sites over the different cortices. We define three bilateral REGIONS to identify overall connectivity: Frontal (F), Centro-temporal (CT), and Parieto-occipital (PO). The Central and Temporal, and Parietal and Occipital channels were combined since the total number of electrodes was low. As an example, the left hemisphere regions are Frontal (Fp1, F7, and F3), Centro-temporal (C3 and T3), and Parieto-occipital (P3 and O1). For the EEG data, CONDITION refers only to the None and 15Hz BB conditions (which will be explained in section 3.2). CHANNELS refers to the 16 individual channels of recorded EEG data. HEMISPHERE refers to the electrodes in the left or right hemispheres.

*2.8.3. Regional Connection Strength Analysis.* The effect of CONDITION (None and 15Hz BB) on the regional connection (LINK) PLV strength was evaluated in a two-way ANOVA. LINK refers to the three anterior - posterior connections (F – CT, F – PO, and CT – PO) for each hemisphere and three bilateral connections (F – F, CT – CT, and PO – PO). The regional links were determined by averaging the regional connections between the clusters of electrodes.

### 3. Results

#### 3.1. N-Back Task Performance

No significant changes due to CONDITION were found for the participants’ reaction time ( $\chi^2(5, 34) = 2.63$ ,  $p = 0.757$ ) nor for the raw accuracy scores ( $\chi^2(5, 34) = 0.59$ ,  $p = 0.968$ ) when compared in a nonparametric Mann-Whitney U statistical test. Table 1 shows the mean accuracy and standard deviation for each condition. Overall, the mean values for the experimental conditions are higher than the control conditions but the differences are not statistically significant due to high variability. The large variance is likely due to the different load levels or larger age range.

Table 1: Mean and Standard Deviation of the Raw Accuracy

| None         | Pure          | Classical    | 5Hz BB       | 10Hz BB      | 15Hz BB       |
|--------------|---------------|--------------|--------------|--------------|---------------|
| 92.95 ± 8.1% | 92.77 ± 11.6% | 93.33 ± 9.2% | 94.39 ± 7.0% | 93.92 ± 7.6% | 94.15 ± 9.5 % |



A nonparametric Mann-Whitney U test showed that the effect of CONDITION on the ranked accuracy was statistically significant ( $\chi^2(5, 34) = 15.07, p = 0.0101$ ). Post hoc pairwise analyses are shown in Figure 2. The only statistically significant result is that, individually, participants' performed significantly better during the 15Hz BB than during the None condition ( $p = 0.0041$ ). The other conditions were not significantly different from either None or 15Hz BB.

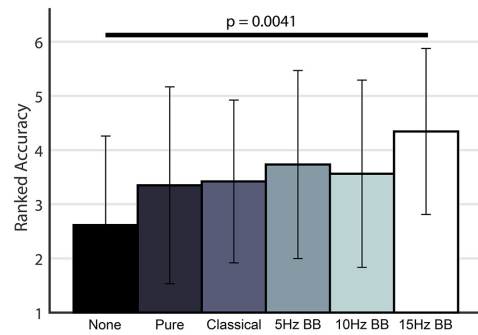


Figure 2: Ranked Accuracy for the six acoustic stimulation conditions.

### 3.2. Frequency Band

The results of the frequency band analysis are shown in Figure 3. The uncorrected t-statistics, comparing the FFT power for the None condition and the three binaural beat conditions, for each channel, are shown in Figure 3A. The results of the two-way factorial ANOVA determined that CONDITION ( $F(3,240) = 15.8, p < 0.0001$ ), BAND ( $F(3,240) = 723.0, p < 0.0001$ ) had significant effects on the mean FFT power but their interaction ( $F(9,240) = 1.8, p = 0.07$ ) did not. Based on Tukey HSD post hoc analysis, the theta band ( $p < 0.0001$ ) and 15Hz BB ( $p < 0.002$ ) were significantly higher over all other frequency bands and conditions, respectively.

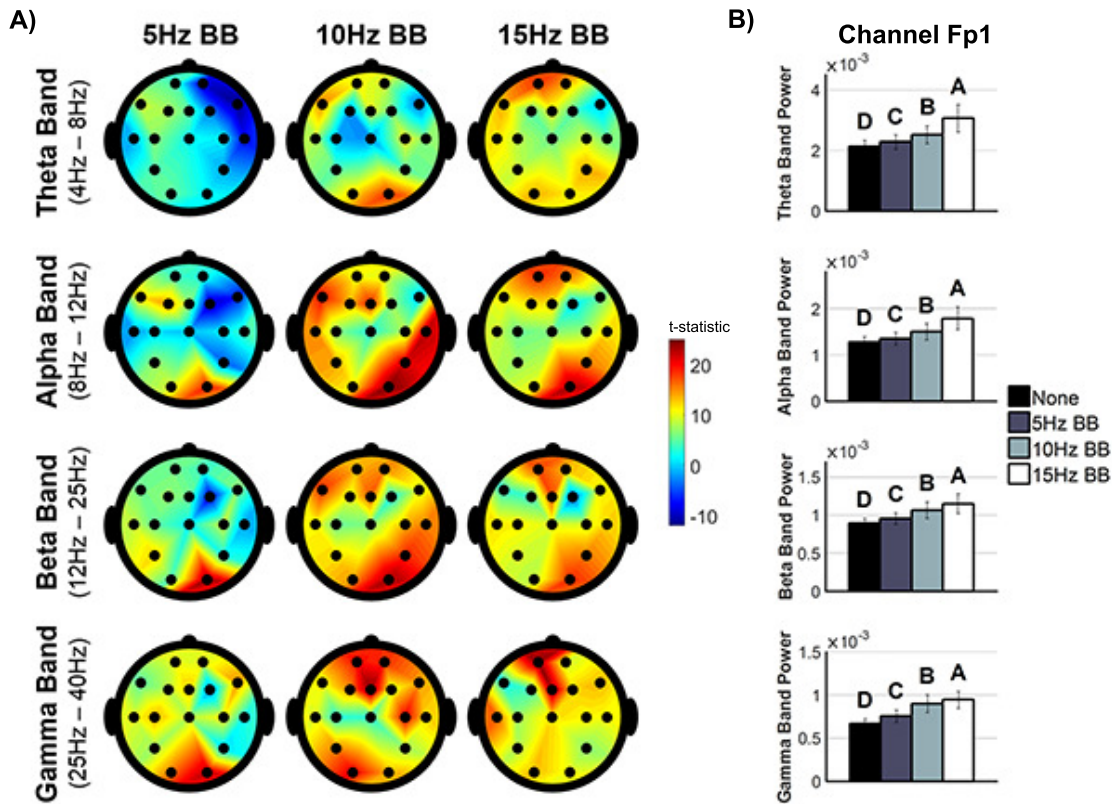


Figure 3: A) The uncorrected t-statistic values comparing the FFT power for None against the binaural stimulation conditions. B) The mean and standard deviation for channel Fp1. Conditions marked with different letters are significantly different. Bars show standard error.

In addition, Figure 3B shows the FFT power for only the left prefrontal electrode (Fp1). Four one-way ANOVAs, one for each frequency band, analyzed the effect of CONDITION on the bootstrapped FFT power. CONDITION was significant for Theta ( $F(3,396) = 165.3, p < 0.0001$ ), Alpha ( $F(3,396) = 165.0, p < 0.0001$ ), Beta ( $F(3,396) = 133.7, p < 0.0001$ ), and Gamma ( $F(3,396) = 230.4, p < 0.0001$ ).

Therefore, based on the behavioral and frequency response results, only the theta band EEG responses for the None and 15Hz BB conditions will be considered for the remaining analysis.

### 3.3. Connectivity Networks

An ANOVA, with the CONDITION as the independent variable, determined that the edge weights of the networks (Figure 4) were significantly higher for 15Hz BB when compared to None ( $F(1,478) = 2.41, p = 0.0163$ ).

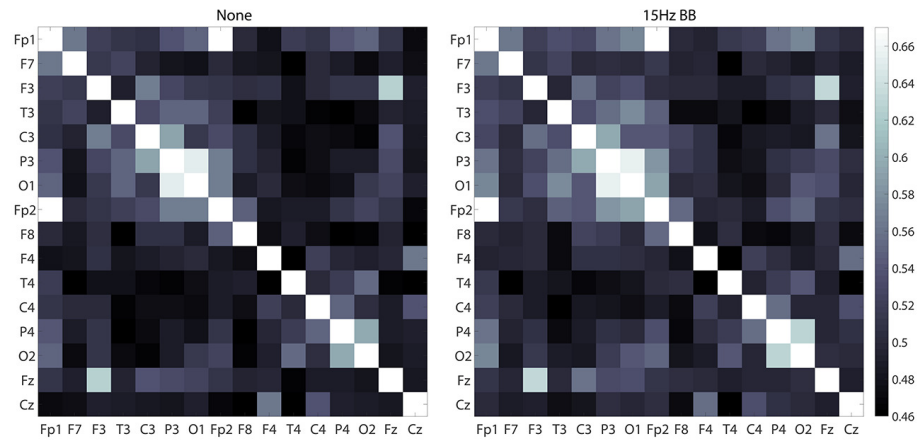


Figure 4: Mean theta weight matrices for the None and 15Hz BB acoustic stimulation conditions averaged over all participants.

### 3.4. Graphical Network Measure

A two-way ANOVA, shown in Figure 5A, was constructed to analyze the effect of CONDITION and CHANNELS on the degree values of the networks shown in Figure 4. CONDITION ( $F(1,3168) = 70.6, p < 0.0001$ ), CHANNELS ( $F(15,3168) = 153.5, p < 0.0001$ ), and their interaction  $CONDITION \times CHANNELS$  ( $F(15,3168) = 3.8, p < 0.0001$ ) were significant. Overall, the degree values are higher for 15Hz BB when compared against None. Figure 5B shows the differences between the two conditions in Figure 5A, topographically, for each channel. The prefrontal, parietal, and occipital channels have the largest positive changes between conditions.

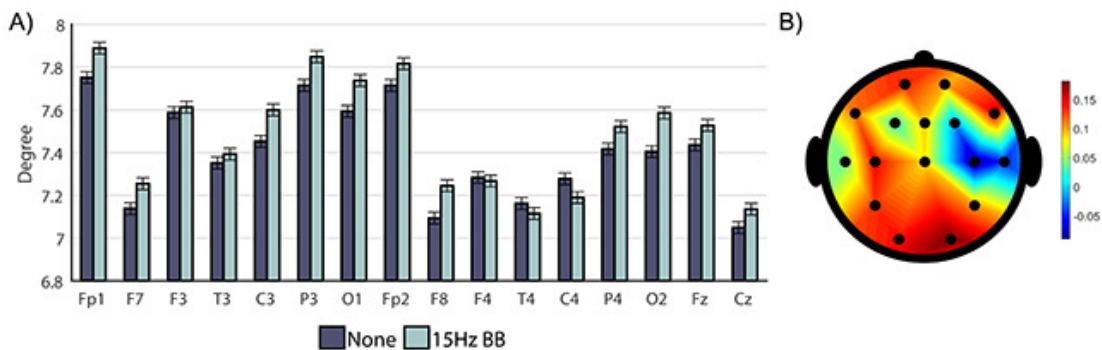


Figure 5: A) Mean degree of nodes in connectivity networks averaged over 100 bootstrapped samples. Bars show standard error. B) Difference between conditions (15Hz BB - None).

Furthermore, three separate two-way ANOVAs, one for each REGION, were constructed to determine the effect of CONDITION and HEMISPHERE on degree, and are shown in Figure 6. Listed on the graph are the F values from each ANOVA (DOF = 2,  $N_F = 1197$ ,  $N_{CT} = 797$ , and  $N_{PO} = 797$ ). Generally, the left hemisphere values are higher than the right.

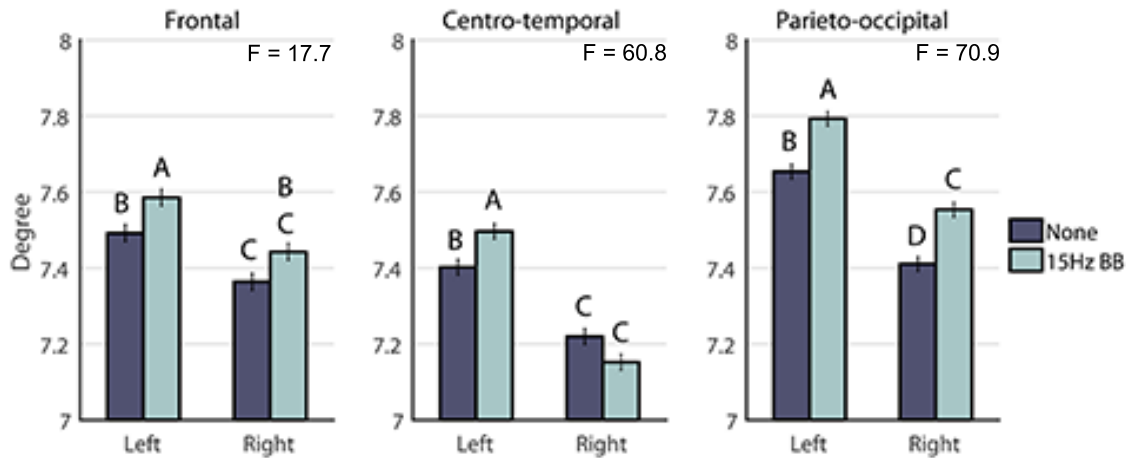


Figure 6: Mean degree for each condition across hemispheres averaged over 100 bootstrapped samples. Conditions marked with different letters are significantly different. Bars show standard error.

### 3.5. Regional Connectivity

A  $2 \times 9$  factorial ANOVA was constructed to compare the effect of LINK and CONDITION on the PLV connection strengths from Figure 4. The main effects of CONDITION ( $F(1,1780) = 71.9$ ,  $p < 0.0001$ ), LINK ( $F(8,1780) = 486.4$ ,  $p < 0.0001$ ), and their interaction  $CONDITION \times LINK$  ( $F(8,1780) = 9.31$ ,  $p < 0.0001$ ) were significant. Figure 7 highlights the differences in link strengths of the networks between those formed when listening to 15Hz BB versus None. Red indicates that the strength increased during 15Hz BB stimulation, and blue shows a decrease. Regions connected by a dotted line produced insignificant changes between conditions. All connections, except for the right centro-temporal to parieto-occipital and interhemispheric centro-temporal connections, increased when listening to 15Hz BB. Most importantly, the 15Hz BB produced significant increases in the bilateral frontoparietal network and left hemispheric connections. Table 2 shows mean and standard deviation of the connection strengths over 100 bootstrapped samples, the mean difference between the two conditions, and the results of the t-tests comparing None to the 15Hz BB for each link.

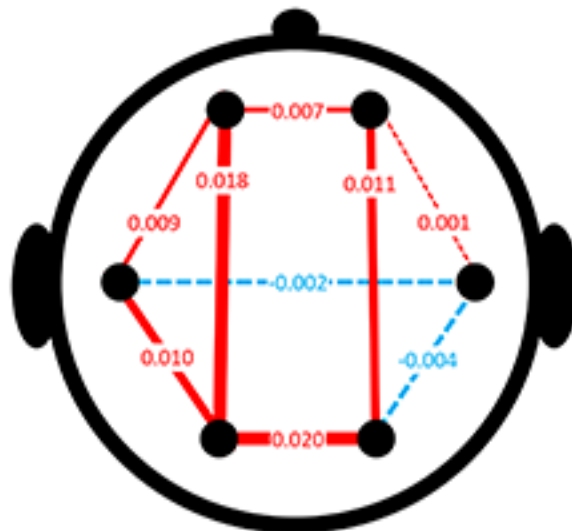


Figure 7: Regional PLV connection strength differences between the None and 15Hz BB conditions.

Table 2: Regional Connections

| Link        | PLV Connection Strength |               | Difference | p-value | t-statistic |
|-------------|-------------------------|---------------|------------|---------|-------------|
|             | None                    | 15Hz BB       |            |         |             |
| PO – PO     | 0.479 ± 0.019           | 0.499 ± 0.016 | 0.020      | < .0001 | 8.25        |
| F – PO (L)  | 0.501 ± 0.027           | 0.519 ± 0.024 | 0.018      | < .0001 | 5.01        |
| F – PO (R)  | 0.477 ± 0.016           | 0.488 ± 0.014 | 0.011      | < .0001 | 5.37        |
| CT – PO (L) | 0.554 ± 0.026           | 0.564 ± 0.024 | 0.010      | 0.005   | 2.84        |
| F – CT (L)  | 0.501 ± 0.024           | 0.510 ± 0.023 | 0.009      | 0.005   | 2.82        |
| F – F       | 0.507 ± 0.017           | 0.514 ± 0.016 | 0.007      | 0.006   | 2.76        |
| CT – PO (R) | 0.526 ± 0.019           | 0.522 ± 0.016 | -0.004     | 0.130   | -1.52       |
| CT – CT     | 0.456 ± 0.019           | 0.454 ± 0.018 | -0.002     | 0.416   | -0.81       |
| F – CT (R)  | 0.470 ± 0.018           | 0.471 ± 0.016 | 0.001      | 0.777   | 0.28        |

#### 4. Discussion

**15Hz binaural beats increases relative accuracy during an N-Back task.** Based on a power analysis, the participant N number was not large enough to determine any significances in raw accuracy scores. However, the ranked accuracy values, shown in Figure 2, produced the key result that, individually, participants performed significantly better overall when listening to 15Hz BB than None. Classical Music and Pure Tone produced an insignificant change from None which is consistent with previous literature [41]. In addition, neither the 5Hz or 10Hz BB produced significant changes from the None condition. The increase in performance when listening to 15Hz BB can be potentially explained by noting that 15Hz BB produced the highest change in the theta band frequency response magnitude, increased the degree of the network in prefrontal and parietal channels, and increased synchronization within the frontoparietal network.

**15Hz binaural beats impacts EEG frequency response magnitude.** As shown in Figure 3, binaural stimulation frequency changes the EEG frequency responses over all channels. The theta (5Hz) BB stimulation responses show that, overall, the frequency power was unchanged or decreased when compared to None, except for within the gamma band. The alpha (10Hz) and beta (15Hz) binaural stimulation frequencies resulted in similar responses across the four bands. However, 15Hz BB produces higher power within the theta band in the left frontal and parietal electrodes. Activation of both regions, within the theta band, is key to working memory performance. Additionally, over all frequency bands, the 15Hz BB produced significantly higher power in the left prefrontal electrode (Fp1) than all other stimulation conditions. Finally, for Fp1, the theta band had the largest change in magnitude between the 15Hz BB and 10Hz BB. These results are consistent with the role of Fp1 in working memory [42].

**15Hz binaural beats modifies network structure.** As shown in Figure 5A, the channels with the highest degree values, in each hemisphere, correspond to the electrodes over the frontal and parieto-occipital cortices. This result is reflected in Figure 5B and Figure 6 which shows that, generally, the frontal and parieto-occipital values are higher than the centro-temporal results. The results shown in Figure 6 agree with [16, 18]

that a verbal working memory task activates both bilateral frontal and parietal regions with additional regions recruited in the left hemisphere. In addition, as shown in both Figure 5 and Figure 6, 15Hz BB increases the degree values in both the left and right hemispheres. **The network of brain activity produced when listening to 15Hz BB, has higher global information transfer than does the baseline network produced by only task performance (no auditory stimulation). The increase in information transfer could explain the change in the behavioral data.**

**15Hz binaural beats changes regional linkages.** 15Hz binaural beats produces the largest change in four links, shown in Figure 7: PO – PO, bilateral F – PO, and left CT – PO. Of all the links, the bilateral parieto-occipital connectivity strength increased the most when compared to the None condition. The parietal cortices are involved with early visual signal processing [43] and visual attention feedback [44]. The letters of the N-Back task are encoded as both visuospatial (right hemisphere) and verbal (left hemisphere) objects. In addition, the bilateral frontoparietal network connectivity strength increased significantly when listening to the 15Hz BB. In previous studies, the interactions between the parietal and prefrontal cortices have been strongly associated with working memory performance [42, 45]. Also, the left hemisphere parieto-occipital to centro-temporal link strength increased. The connection between these two regions is associated with verbal working memory in the form of phonological storage and subvocal rehearsal of the information [13, 46]. Synthesizing these results, we see that the 15Hz BB influences the most important links used within the working memory network which could explain the benefited performance we observe.

## 5. Conclusion

This study demonstrates that listening to 15Hz binaural beats can affect cortical network properties during a verbal working memory task. The network produced when listening to 15Hz binaural beats indicates more information transfer than that produced when listening to no sound. Also, the frontoparietal bilateral network increased significantly in connectivity when listening to the 15Hz binaural beats. Furthermore, only the 15Hz binaural beats condition produced significantly more accurate responses, in individuals, when compared to listening to no sound. The other acoustic stimulation conditions produced no significant changes. Therefore, these results indicate that 15Hz binaural beats can be used to change the frequency response and connectivity of cortical networks, and thereby influence verbal working memory task performance.

Future experiments should focus on determining the nonlinear relationship between the binaural beat stimuli and the observed cortical activity and behavior. From previous experiments, it has been shown that 40Hz BB produces maximal responses. If 40Hz BB had been included with the battery of binaural stimulation frequencies tested, then it potentially might have produced the highest cortical frequency response. However, it is unknown if it would have produced the desired changes in the behavior, which should be explored.

## 6. References

- [1] Sporns O. *Networks of the Brain*. MIT press; 2011.

- [2] Park HJ, Friston K. Structural and functional brain networks: from connections to cognition. *Science*. 2013;342(6158):1238411.
- [3] Kanagasabapathi TT, Massobrio P, Barone RA, Tedesco M, Martinoia S, Wadman WJ, et al. Functional connectivity and dynamics of cortical-thalamic networks co-cultured in a dual compartment device. *Journal of Neural Engineering*. 2012;9(3):036010.
- [4] So K, Koralek AC, Ganguly K, Gastpar MC, Carmena JM. Assessing functional connectivity of neural ensembles using directed information. *Journal of Neural Engineering*. 2012;9(2):026004.
- [5] Fraschini M, Demuru M, Crobe A, Marrosu F, Stam CJ, Hillebrand A. The effect of epoch length on estimated EEG functional connectivity and brain network organisation. *Journal of Neural Engineering*. 2016;13(3):036015.
- [6] Kuramoto Y. *Chemical Oscillations, Waves, and Turbulence*. vol. 19. Springer Science & Business Media; 2012.
- [7] Varela F, Lachaux JP, Rodriguez E, Martinerie J. The brainweb: phase synchronization and large-scale integration. *Nature Reviews Neuroscience*. 2001;2(4):229–239.
- [8] Buzsáki G, Draguhn A. Neuronal oscillations in cortical networks. *Science*. 2004;304(5679):1926–1929.
- [9] Sauseng P, Klimesch W, Doppelmayr M, Hanslmayr S, Schabus M, Gruber WR. Theta coupling in the human electroencephalogram during a working memory task. *Neuroscience Letters*. 2004;354(2):123–126.
- [10] Jensen O, Kaiser J, Lachaux JP. Human gamma-frequency oscillations associated with attention and memory. *Trends in Neurosciences*. 2007;30(7):317–324.
- [11] Moran RJ, Campo P, Maestu F, Reilly RB, Dolan RJ, Strange BA. Peak frequency in the theta and alpha bands correlates with human working memory capacity. *Frontiers in Human Neuroscience*. 2010;4:200.
- [12] Baddeley AD, Hitch GJ. Working memory. *The Psychology of Learning and Motivation*. 1974;8:47–89.
- [13] Baddeley A. The episodic buffer: a new component of working memory? *Trends in Cognitive Sciences*. 2000;4(11):417–423.
- [14] Fell J, Axmacher N. The role of phase synchronization in memory processes. *Nature Reviews Neuroscience*. 2011;12(2):105–118.
- [15] Jutras MJ, Buffalo EA. Synchronous neural activity and memory formation. *Current Opinion in Neurobiology*. 2010;20(2):150–155.
- [16] Ray MK, Mackay CE, Harmer CJ, Crow TJ. Bilateral generic working memory circuit requires left-lateralized addition for verbal processing. *Cerebral Cortex*. 2008;18(6):1421–1428.
- [17] Owen AM, McMillan KM, Laird AR, Bullmore E. N-back working memory paradigm: A meta-analysis of normative functional neuroimaging studies. *Human Brain Mapping*. 2005;25(1):46–59.
- [18] Dima D, Jogia J, Frangou S. Dynamic causal modeling of load-dependent modulation of effective connectivity within the verbal working memory network. *Human Brain Mapping*. 2014;35(7):3025–3035.
- [19] Sarnthein J, Petsche H, Rappelsberger P, Shaw G, Von Stein A. Synchronization between prefrontal and posterior association cortex during human working memory. *Proceedings of the National Academy of Sciences*. 1998;95(12):7092–7096.
- [20] Smith EE, Jonides J. Storage and executive processes in the frontal lobes. *Science*. 1999;283(5408):1657–1661.
- [21] Fitzpatrick DC, Roberts JM, Kuwada S, Kim DO, Filipovic B. Processing temporal modulations in binaural and monaural auditory stimuli by neurons in the inferior colliculus and auditory cortex. *Journal of the Association for Research in Otolaryngology*. 2009;10(4):579–593.
- [22] Scott BH, Malone BJ, Semple MN. Representation of dynamic interaural phase difference in auditory cortex of awake rhesus macaques. *Journal of Neurophysiology*. 2009;101(4):1781–1799.
- [23] Oster G. Auditory beats in the brain. *Scientific American*. 1973;229(4):94–102.
- [24] Spitzer MW, Semple MN. Transformation of binaural response properties in the ascending auditory pathway: influence of time-varying interaural phase disparity. *Journal of Neurophysiology*. 1998;80(6):3062–3076.
- [25] Draganova R, Ross B, Wollbrink A, Pantev C. Cortical steady-state responses to central and peripheral auditory beats. *Cerebral Cortex*. 2008;18(5):1193–1200.

- [26] Pastor MA, Artieda J, Arbizu J, Marti-Climent JM, Peñuelas I, Masdeu JC. Activation of human cerebral and cerebellar cortex by auditory stimulation at 40 Hz. *The Journal of Neuroscience*. 2002;22(23):10501–10506.
- [27] Ross B, Miyazaki T, Thompson J, Jamali S, Fujioka T. Human cortical responses to slow and fast binaural beats reveal multiple mechanisms of binaural hearing. *Journal of Neurophysiology*. 2014;112(8):1871–1884.
- [28] Schwarz DW, Taylor P. Human auditory steady state responses to binaural and monaural beats. *Clinical Neurophysiology*. 2005;116(3):658–668.
- [29] Chaieb L, Wilpert EC, Reber TP, Fell J. Auditory beat stimulation and its effects on cognition and mood states. *Frontiers in Psychiatry*. 2015;6.
- [30] Gao X, Cao H, Ming D, Qi H, Wang X, Wang X, et al. Analysis of EEG activity in response to binaural beats with different frequencies. *International Journal of Psychophysiology*. 2014;94(3):399–406.
- [31] Lane JD, Kasian SJ, Owens JE, Marsh GR. Binaural auditory beats affect vigilance performance and mood. *Physiology & Behavior*. 1998;63(2):249–252.
- [32] Beauchene C, Abaid N, Moran R, Diana RA, Leonessa A. The Effect of Binaural Beats on Visuospatial Working Memory and Cortical Connectivity. *PloS ONE*. 2016;11(11):e0166630.
- [33] Homan RW, Herman J, Purdy P. Cerebral location of international 10–20 system electrode placement. *Electroencephalography and Clinical Neurophysiology*. 1987;66(4):376–382.
- [34] Vogel EK, McCollough AW, Machizawa MG. Neural measures reveal individual differences in controlling access to working memory. *Nature*. 2005;438(7067):500–503.
- [35] Delorme A, Makeig S. EEGLAB: an open source toolbox for analysis of single-trial EEG dynamics including independent component analysis. *Journal of Neuroscience Methods*. 2004;134(1):9–21.
- [36] Makeig S, Bell AJ, Jung TP, Sejnowski TJ, et al. Independent component analysis of electroencephalographic data. *Advances in neural information processing systems*. 1996;p. 145–151.
- [37] Lachaux JP, Rodriguez E, Martinerie J, Varela FJ, et al. Measuring phase synchrony in brain signals. *Human Brain Mapping*. 1999;8(4):194–208.
- [38] Selesnick IW. The design of approximate Hilbert transform pairs of wavelet bases. *IEEE Transactions on Signal Processing*. 2002;50(5):1144–1152.
- [39] Ioannou CI, Pereda E, Lindsen JP, Bhattacharya J. Electrical brain responses to an auditory illusion and the impact of musical expertise. *PloS ONE*. 2015;10(6):e0129486.
- [40] Luan B, Sörös P, Sejdić E. A study of brain networks associated with swallowing using graph-theoretical approaches. *PloS ONE*. 2013;8(8):e73577.
- [41] Kmpfe J, Sedlmeier P, Renkewitz F. The impact of background music on adult listeners: A meta-analysis. *Psychology of Music*. 2010;.
- [42] Curtis CE, D’Esposito M. Persistent activity in the prefrontal cortex during working memory. *Trends in Cognitive Sciences*. 2003;7(9):415–423.
- [43] Nakashita S, Saito DN, Kochiyama T, Honda M, Tanabe HC, Sadato N. Tactile–visual integration in the posterior parietal cortex: A functional magnetic resonance imaging study. *Brain Research Bulletin*. 2008;75(5):513–525.
- [44] Brown H, Friston K. The functional anatomy of attention: a DCM study. *Frontiers in Human Neuroscience*. 2013;7(784).
- [45] Postle BR. Working memory as an emergent property of the mind and brain. *Neuroscience*. 2006;139(1):23–38.
- [46] Nixon P, Lazarova J, Hodinott-Hill I, Gough P, Passingham R. The inferior frontal gyrus and phonological processing: an investigation using rTMS. *Journal of Cognitive Neuroscience*. 2004;16(2):289–300.